AGU PUBLICATIONS

Geophysical Research Letters

RESEARCH LETTER
10.1002/2015GL063363

Key Points:
- Tropical rainforest response to marine sky brightening is investigated in three ESMs
- Two models show GPP reduction from geoengineering, one Amazon dieback reversal
- Possibly adverse effects on plants and soils from salt of this geoengineering type

Supporting Information:
- Figure S1, Texts S1–S5, and Tables 1 and 2

Correspondence to:
H. Muri,
helene.muri@gmail.com

Citation:
Muri, H., U. Niemeier, and J. E. Kristjánsson (2015), Tropical rainforest response to marine sky brightening climate engineering, *Geophys. Res. Lett.*, *42*, 2951–2960, doi:10.1002/2015GL063363.

Received 5 FEB 2015
Accepted 23 MAR 2015
Accepted article online 24 MAR 2015
Published online 16 APR 2015

Tropical rainforest response to marine sky brightening climate engineering

Helene Muri[1], Ulrike Niemeier[2], and Jón Egill Kristjánsson[1]

[1]Department of Geosciences, University of Oslo, Oslo, Norway, [2]Max Planck Institute for Meteorology, Hamburg, Germany

Abstract Tropical forests represent a major atmospheric carbon dioxide sink. Here the gross primary productivity (GPP) response of tropical rainforests to climate engineering via marine sky brightening under a future scenario is investigated in three Earth system models. The model response is diverse, and in two of the three models, the tropical GPP shows a decrease from the marine sky brightening climate engineering. Partial correlation analysis indicates precipitation to be important in one of those models, while precipitation and temperature are limiting factors in the other. One model experiences a reversal of its Amazon dieback under marine sky brightening. There, the strongest partial correlation of GPP is to temperature and incoming solar radiation at the surface. Carbon fertilization provides a higher future tropical rainforest GPP overall, both with and without climate engineering. Salt damage to plants and soils could be an important aspect of marine sky brightening.

1. Introduction

Tropical rainforests comprise an essential component of the global carbon cycle and account for the largest atmosphere-to-land carbon flux [*Beer et al.*, 2010]: hence, its fate in the future is of vital importance. It occurs mainly between 10°S and 10°N, with temperatures between 20 and 30°C yr round and abundant precipitation, of the order of 1500–4300 mm yr^{-1} [*Whittaker*, 1975]. The largest coverage is in the Americas, followed by Africa, equatorial Asia. Limiting factors for plant growth include water availability (precipitation and water vapor), nutrient supply, temperature, CO_2, and sunlight for photosynthesis [*Boer and Arora*, 2010; *Piao et al.*, 2009; *Rutishauser et al.*, 2011; *Wolkovich et al.*, 2012]. While tropical temperatures are predicted to increase over this century, the regional water availability projections are more uncertain [e.g., *Cook and Vizy*, 2006; *Kitoh et al.*, 2013].

Over the past five decades, 25–30% of anthropogenic CO_2 emissions have been absorbed by the terrestrial ecosystem [*Le Quéré et al.*, 2009, 2014], with ~18% absorbed by tropical forests [*Lewis et al.*, 2009]. Elevated atmospheric carbon concentrations enable higher carbon uptake by plants ("carbon fertilization") [*Norby et al.*, 2005]. Moreover, stomata are narrowed [*Field et al.*, 1995], increasing the water use efficiency as the transpiration rates are reduced. Short-term observations have shown an increase in carbon storage in plants and soils with increasing CO_2 emissions [*Norby et al.*, 2005; *Nowak et al.*, 2004]. However, the terrestrial biosphere's carbon uptake capacity might be reduced with time when changes to other variables, like water availability, dry season length, temperatures, and sunlight, are accounted for [*Dukes et al.*, 2005; *Norby et al.*, 2010; *Shaw et al.*, 2002]. The C^4MIP (Coupled Climate-Carbon Cycle Model Intercomparison Project) ensemble showed that future climate change might reduce the Earth system's efficiency in absorbing CO_2 and that a larger fraction anthropogenic emissions will stay airborne [*Friedlingstein et al.*, 2006; *Canadell et al.*, 2007]. A major reduction in the carbon uptake was attributed to the tropical land areas.

Due to the current stalemate in climate policy, climate engineering—or geoengineering—has been introduced as a potential option alongside mitigation and adaptation. Climate engineering can be defined as the deliberate modification of the climate in order to alleviate negative effects of anthropogenic climate change. One of the discussed techniques involves cooling the climate by increasing the Earth's reflectivity via brightening of clouds [e.g., *Latham*, 1990; *Korhonen et al.*, 2010; *Jones and Haywood*, 2012]. The method is referred to as marine cloud/sky brightening, or sea spray climate engineering. The idea is to inject naturally occurring sea salt into low-level clouds and cloud forming regions over the oceans. This would lead to more numerous and smaller cloud droplets than in unseeded clouds, resulting in a higher cloud albedo (aerosol indirect effect). This way more solar radiation is reflected by the clouds and a cooling ensues. Additionally, the sea salt aerosols themselves could contribute toward reflection of solar radiation (direct effect).

This work investigates the effect of marine sky brightening (MSB) on the carbon fluxes from the atmosphere to the terrestrial biosphere in tropical rainforests in three Earth system models. So far, merely a few studies with just one model have looked at the vegetation carbon uptake capacity change under marine cloud brightening [*Jones and Haywood*, 2012; *Jones et al*., 2009, 2011]. *Jones et al*. [2009] found that the African tropical productivity was somewhat increased and there was little change in the Asian tropical forest in the HadGEM model. The changes in the net carbon uptake by the vegetation were attributed to precipitation changes. The sign of change and magnitude to the Amazon net primary productivity varied depending on the experiment design [*Jones and Haywood*, 2012; *Jones et al*., 2009, 2011]. A multimodel approach is needed to detect any robust features of primary productivity change from MSB, which is attempted in this work.

Section 2 presents the method and models used, section 3 the results, while conclusions are drawn in section 4.

2. Method

2.1. The Models

Three Earth system models were used in this work: NorESM1-M [*Bentsen et al*., 2013], IPSL-CM5A-LR [*Dufresne et al*., 2013], and MPI-ESM-LR [*Giorgetta et al*., 2013]. The models were chosen as they are structurally different, which increases the confidence in any robust features expressed by all three models. These fully coupled climate models run atmosphere and vegetation models at the same horizontal resolution, as detailed below. The models define plant functional types (PFTs) based on plant phenology type, physiognomy, photosynthetic pathway, and climate zone [e.g., *Poulter et al*., 2011; *Bonan et al*., 2002]. In this study, the tropical broadleaf evergreen tree PFT is considered. The PFTs used by the models are listed in supporting information Text S5.

Community Land Model version 4 (CLM4) [*Oleson et al*., 2010; *Lawrence et al*., 2011] is the vegetation model in NorESM1-M, which includes the nitrogen cycle. The partitioning of shortwave radiation into direct and diffuse is accounted for. Photosynthesis is more efficient under diffuse rather than direct radiation [*Mercado et al*., 2009]. Carbon cycling in the vegetation and ocean is included in NorESM1-M, though it is not interactive with the atmosphere. The land component is run at a horizontal resolution of 1.9° latitude × 2.5° longitude. The vegetation cover is prescribed and updated yearly following the Representative Concentration Pathway 4.5 (RCP4.5) scenario [*Hurtt et al*., 2011].

Organizing Carbon and Hydrology in Dynamic Ecosystems (ORCHIDEE) is the IPSL-CM5A-LR vegetation model [*Krinner et al*., 2005], run at a 2.5° latitude and 3.75° longitude resolution. It models the terrestrial carbon cycle and vegetation state dynamically, while the PFT distribution is prescribed [*Dufresne et al*., 2013]. The model includes carbon assimilation, carbon allocation, and senescence. No distinction is being made between direct and diffuse radiation.

In MPI-ESM-LR, the Joint Scheme for Biosphere Atmosphere Coupling in Hamburg (JSBACH) land model describes physical and biogeochemical aspects of soil and vegetation [*Raddatz et al*., 2007]. The horizontal resolution is 1.9°. The effect of diffuse light on photosynthesis is included.

The terrestrial carbon cycle in the Coupled Model Intercomparison Project Phase 5 (CMIP5) models have been evaluated by *Anav et al*. [2013]. There are no direct measurements of gross primary productivity (GPP), but it has been estimated based on upscaled data from the Flux Network (FLUXNET) of eddy covariance towers [*Beer et al*., 2010]. Most of the models overestimate GPP, both globally and in the tropics. IPSL-CM5A-LR and MPI-ESM-LR overestimate tropical GPP by 15 and 18 kg C m^{-2} yr^{-1}, respectively, compared to the 1985–2005 FLUXNET-derived estimate of ~67 kg C m^{-2} yr^{-1}. NorESM1-M is closer to this with a GPP of 75 kg C m^{-2} yr^{-1}. The modeled temperatures and precipitation are compared to observations in supporting information Table S1.

2.2. The Experiments

Two experiments are analyzed in this study:

1. RCP4.5: Representative Concentration Pathway 4.5, where the total radiative forcing reaches 4.5 W m^{-2} in year 2100, following the CMIP5 protocol [*Taylor et al*., 2011] (see *Kravitz et al*. [2011] for justification).
2. G3-seaSalt: follows the experiment design of Geoengineering Model Intercomparison Project (GeoMIP) G3 [*Kravitz et al*., 2011], except employing marine sky brightening over the ocean at tropical latitudes (30°S–30°N) instead of stratospheric sulfur injections. The climate engineering is applied to a RCP4.5

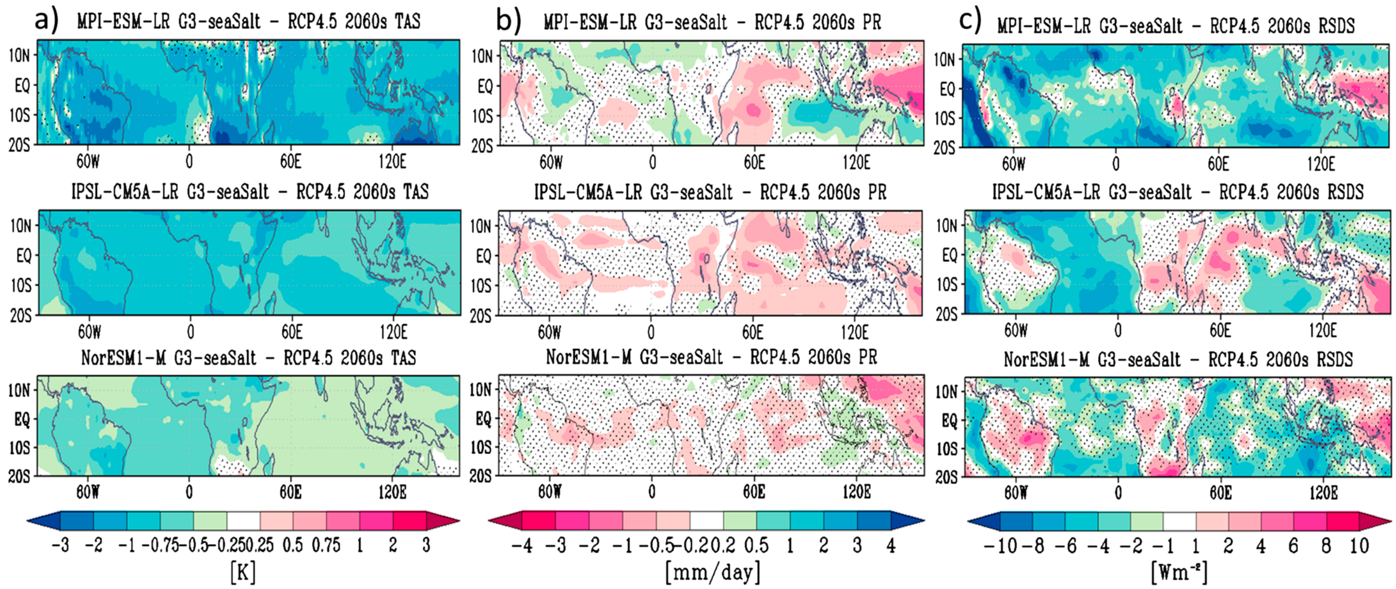

Figure 1. Differences in (a) surface air temperature (K), (b) precipitation rate (PR) (mm d^{-1}), and (c) incoming solar radiation at the surface (RSDS) (W m^{-2}) between G3-seaSalt and RCP4.5 in the 2060s. Nonstippling indicates a confidence level higher than 95%.

background in the period 2020–2070, counteracting increased radiative forcing from greenhouse gases by MSB, keeping the net forcing at 2020 levels. Sea salt is emitted in NorESM1-M, and the simulated distribution is prescribed in MPI-ESM-LR and IPSL-CM5A-LR. Both the direct and the indirect effects of the sea salt particles are included via scattering of shortwave radiation by the sea salt particles and increased cloud albedo in all three models. See *Alterskjær et al*. [2013] for a detailed description of the experiment design.

The last decade of climate engineering is used in the analysis, i.e., 2060–2070 (denoted "2060s"), in addition to the first decade of the RCP4.5 runs, i.e., 2006–2016 ("2010s"). (See supporting information on simulation realization availability.) The statistical significance of the results throughout was found using a Student's *t* test with a *p* value of 0.05.

3. Results

An overview of the results from the G3-seaSalt experiments is presented in *Alterskjær et al*. [2013]. Some additional information is found in the supporting information. Here we focus specifically on the simulated changes in carbon uptake in tropical rainforest areas: South America (Amazon basin), Africa (Congo basin), and Southeast Asia (the tropical islands between the Indian and Pacific Oceans). Annual means are representative due to the relatively small seasonal cycle at these tropical latitudes [*Jung et al*., 2011]. The ratio of NPP (net primary productivity) to GPP can be seen as an estimate of the carbon use efficiency of the ecosystem and is expected to remain the same in a number of CO_2 and temperature scenarios [e.g., *Cheng et al*., 2000; *Tjoelker et al*., 1999], which is found to be the case for the G3-seaSalt and RCP4.5 simulations.

Relevant carbon fluxes and stores are defined as follows:

1. GPP: Gross primary productivity (kg C m^{-2} yr^{-1}) is the gross carbon flux from the atmosphere to land, i.e., the uptake of carbon in photosynthesis.
2. Ra: Autotrophic respiration (kg C m^{-2} yr^{-1}) is the sum of maintenance and growth respiration. Maintenance respiration is the energy attained from photosynthesis used to maintain and repair living biomass. Growth respiration indicates the amount of energy used for construction of new biomass.
3. NPP: Net primary productivity = GPP − Ra (kg C m^{-2} yr^{-1}) is the net flux of carbon from the atmosphere into plants per unit time.
4. cStore: Total carbon storage (kg C m^{-2}) is the carbon content in the terrestrial biosphere, including soil and vegetation.

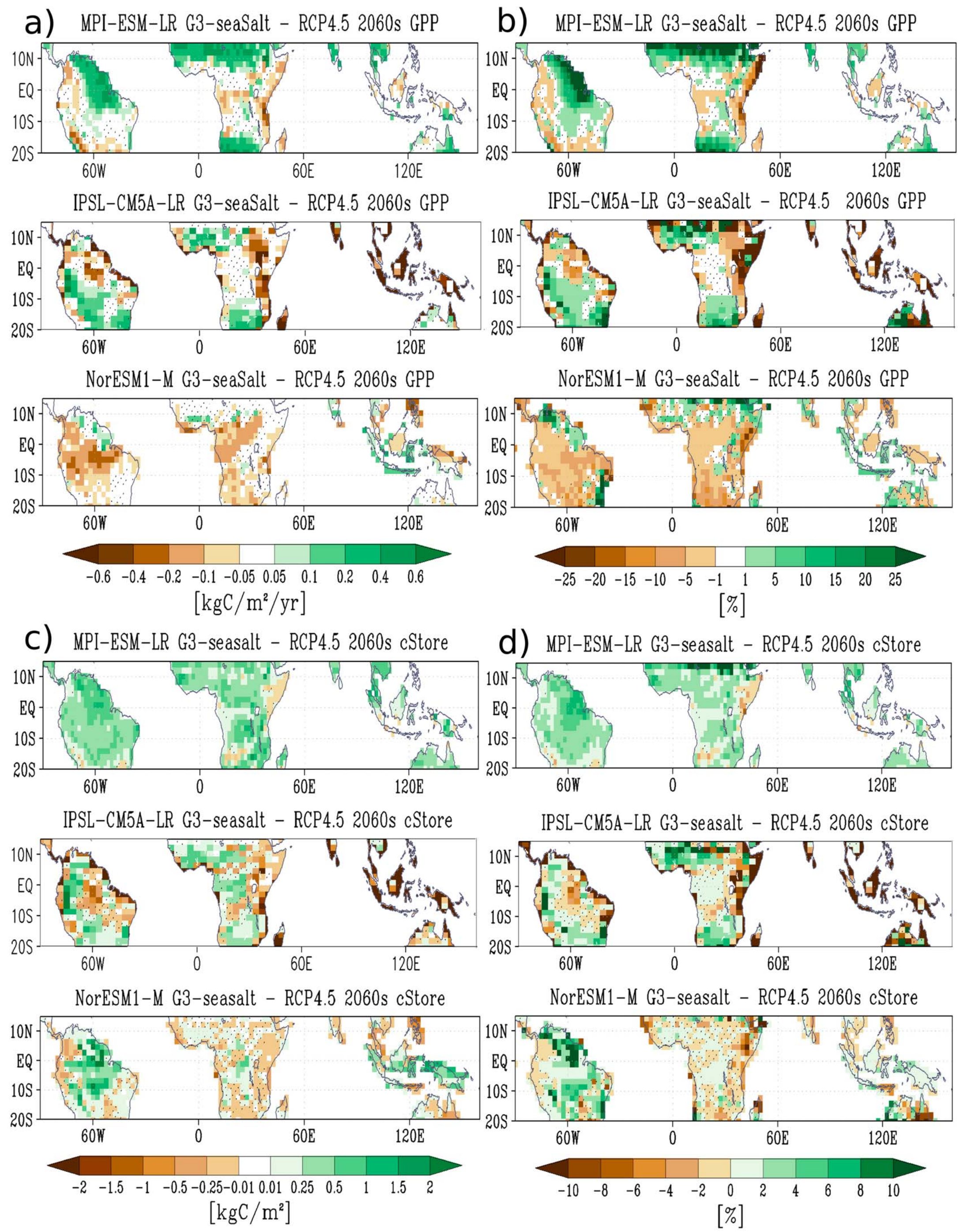

Figure 2. GPP differences between G3-seaSalt and RCP4.5 in the 2060s (a) kg C m^{-2} yr^{-1} and (b) %. The changes in the total carbon storage (cStore), including vegetation and soil, (c) kg C m^{-2} and (d) %, respectively. Nonstippling indicates a confidence level higher than 95%.

3.1. Tropical Response in the Marine Sky Brightening Scenario

All three models show cooling (Figure 1a) in G3-seaSalt compared to RCP4.5 in the 2060s. This is strongest in MPI-ESM-LR with −2 K to −3 K in parts of the Amazon. IPSL-CM5A-LR and NorESM1-M show a decrease in the precipitation (column b) over the tropical rainforests, except Asia in NorESM1-M. The areas with reduced precipitation also have an increase in the surface incoming solar radiation (RSDS) (Figure 1c). MPI-ESM-LR shows an increase in precipitation over Amazon under MSB from changes in the atmospheric circulation (see supporting information) [*Alterskjær et al.*, 2013; *Niemeier et al.*, 2013].

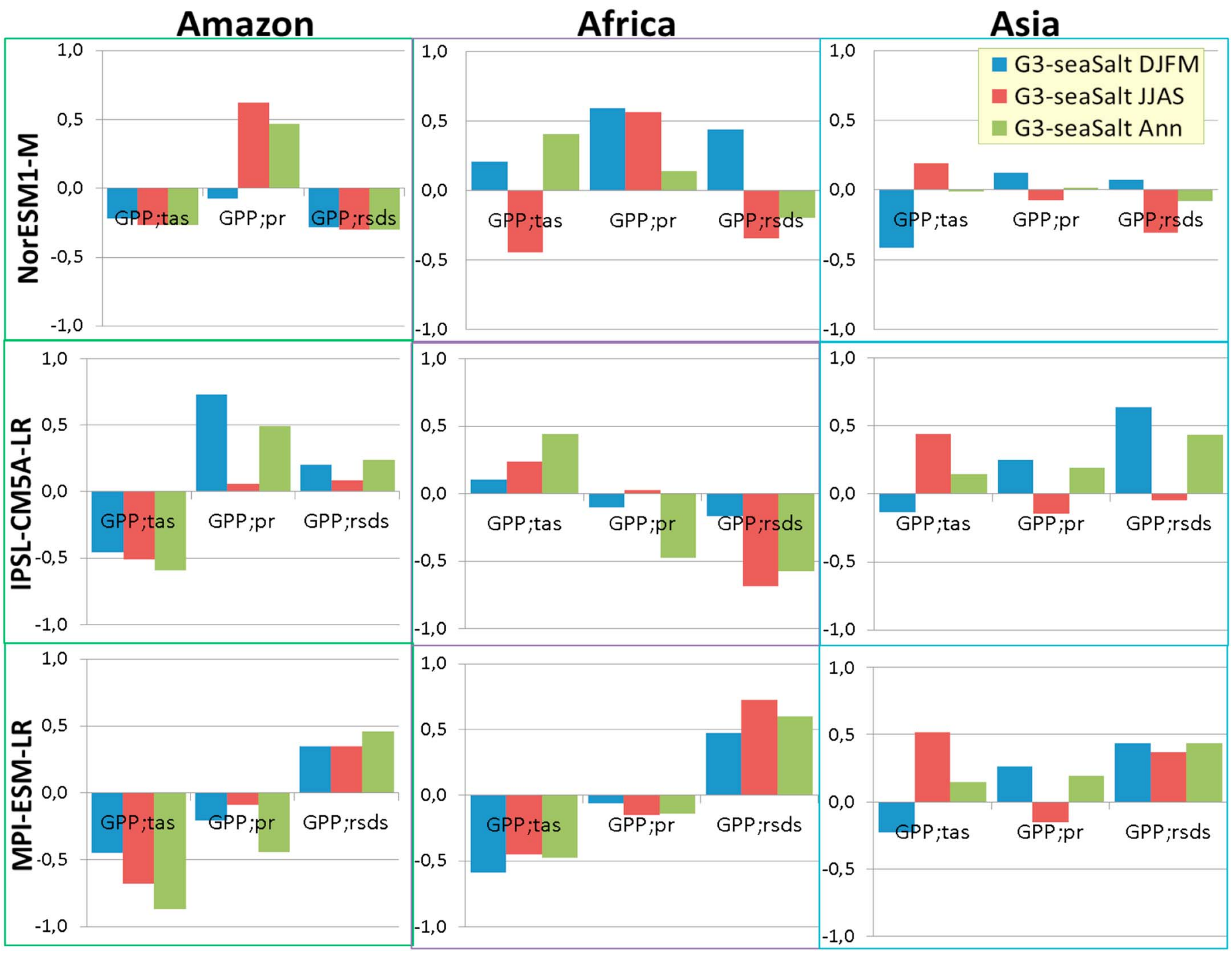

Figure 3. The partial correlation between GPP and three important climatic variables, tas (surface air temperature), pr (precipitation rate), and rsds (surface downwelling shortwave radiation) for the three models over the three regions in the 2060s. Blue bars represent the wet season, here defined as December-January-February-March (DJFM), red bars dry season, June-July-August-September (JJAS), and green bars annual means.

There is an increase in the Amazon forest GPP in the 2060s under MSB in MPI-ESM-LR (Figure 2). IPSL-CM5A-LR has a GPP increase in south-southwestern Amazon of 0.1 to 0.4 kg C m^{-2} yr^{-1}, where the temperatures are cooled the most in the climate engineering simulation (Figure 2). All three models have regions with a reduction in GPP in the 2060s. The reduction is most widespread in NorESM1-M and IPSL-CM5A-LR, with magnitudes of 1–5% over the Amazon and parts of Africa. Some grid boxes have reductions of as much as −10 to −15% (−0.2 to −0.4 kg C m^{-2} yr^{-1}) in NorESM1-M and −15 to −20% in IPSL-CM5A-LR (−0.2 to −0.6 kg C m^{-2} yr^{-1}). The areas with a reduction in precipitation and increase in RSDS have reduced GPP values, indicating water availability as a contributing limiting factor. IPSL-CM5A-LR indicates detrimental effects on the rainforest's carbon drawdown in Asia. It should be noted that this region is hard to simulate well, due to the climate being influenced by the surrounding ocean and land—sea masking in the models.

The relative changes in the total carbon storage (vegetation and soils) are smaller than for GPP in the 2060s (Figure 2). MPI-ESM-LR has higher carbon stocks across the tropics in the MSB case (Figures 2c and 2d). IPSL-CM5A-LR, on the other hand, has a reduction in parts of the Amazon and Asia, which in combination with the GPP reduction implies a shortened residence time of the carbon in the terrestrial ecosystem. NorESM1-M shows small changes in carbon storage in Africa and Asia, and some increases in the Amazon.

10.1002/2015GL063363

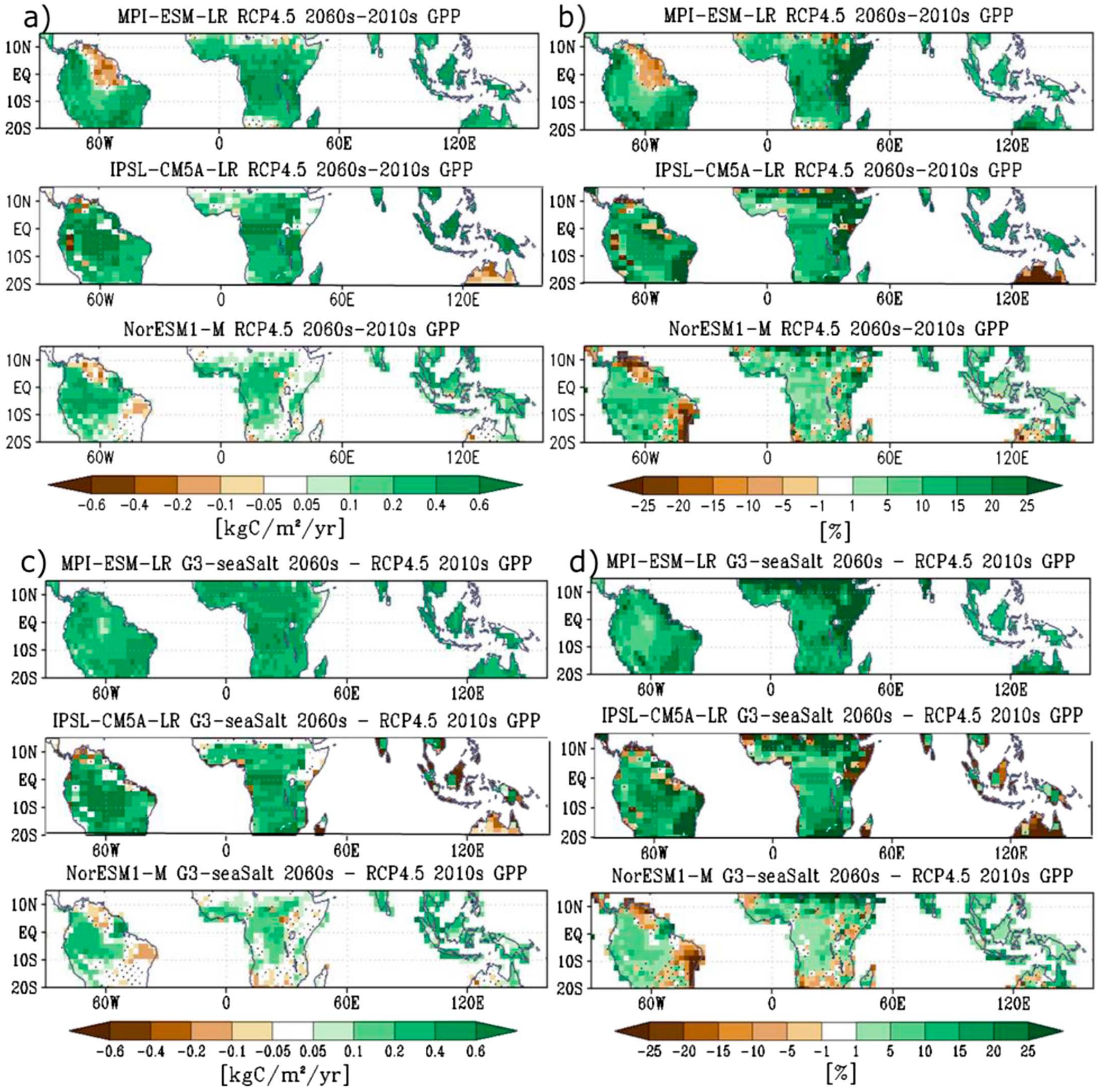

Figure 4. GPP changes relative to RCP4.5 2010s: (a and b) RCP4.5 2060s, (c and d) G3-seaSalt 2060s. Figures 4 and 4c have units kg C m^{-2} yr^{-1}, and Figures 4b and 4d have units %. Nonstippling indicates a confidence level higher than 95%.

Even though the flux of carbon from the atmosphere is reduced, it takes longer for the absorbed carbon to be rereleased to the atmosphere. The cooling from the MSB could be contributing toward longer residence times and protecting the carbon stocks from any further decreases in GPP. There remain large uncertainties with regard to the role of roots and microbial ecology in soil carbon storage, limiting the models ability to reliable forest productivity, relevant biogeochemical processes, and turnover times [e.g., *Norby and Zak*, 2011; *Phillips et al*., 2012].

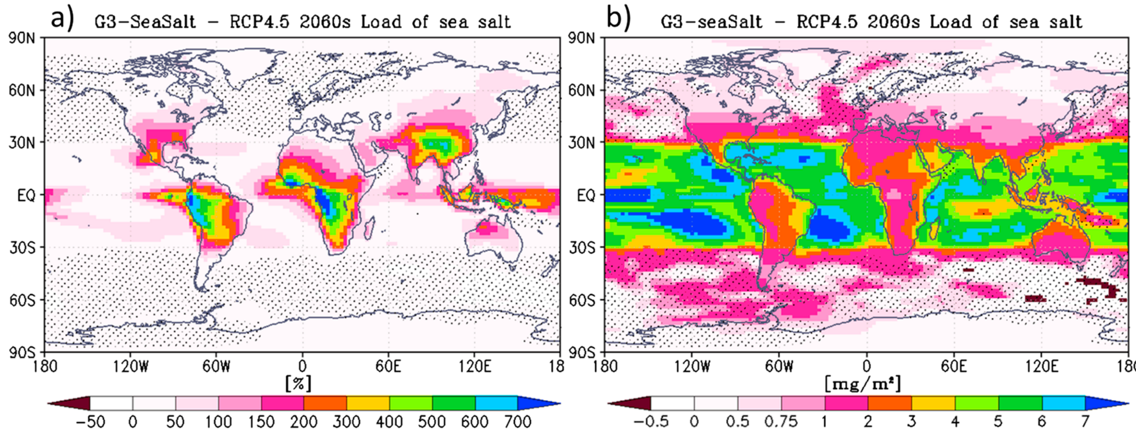

Figure 5. Increase in sea salt load in the lowest atmospheric model level in the 2060s in G3-seaSalt compared to RCP4.5 in NorESM1-M. (a) The relative change (%) and (b) the absolute change (mg m^{-2}). Nonstippling indicates a confidence level higher than 95%.

3.2. Partial Correlation of GPP and Key Climatic Variables

To further investigate the relative importance of the precipitation, temperature, and incoming solar radiation at the surface to GPP, the partial correlation (explanation in supporting information) was calculated for the G3-seaSalt scenario for the wet season, dry season, and annually for the 2060s (Figure 3). There is a great diversity in the model response, although all three models show a negative correlation between GPP and temperature in the Amazon during the dry, wet season, and annually. Lower temperatures are associated with lower evapotranspiration rates and could enhance water availability and affect GPP positively. RSDS shows positive partial correlations to GPP during the dry season in MPI-ESM-LR. Observations have indeed shown that light is a key limiting growth factor in the Amazon dry season [*Huete et al.*, 2006; *Saleska et al.*, 2007]. Besides the indirect effect of temperature and radiation on vegetation, there is the direct effect of heat stress and increased diffuse radiation in relation to lower shortwave radiation levels [*Mercado et al.*, 2009]. During the wet season, precipitation has strong positive partial correlation to GPP in IPSL-CM5A in the Amazon, and in Africa in NorESM1-M. IPSL-CM5A-LR does not account for diffuse radiation in the photosynthesis parameterization; hence, the response of GPP to RSDS is not entirely realistically simulated. Increases in the diffuse fraction of radiation from more aerosol scattering have been shown to improve the efficiency of photosynthesis [*Mercado et al.*, 2009]. There is little agreement among the models as to which climatic variable is the most important for rainforest productivity in Asia and the correlations are weak, suggesting that other factors could be important.

3.3. GPP in the 2060s Compared to "Today"

GPP changes in the 2060s compared to 2010s in the RCP4.5 scenario in Asia and Africa show an increase of up to 0.6 kg C m^{-2} yr^{-1} (Figure 4a), corresponding to 10–20% (Figure 4b). The Amazon, however, shows signs of a degradation of its biomass carrying capacity, or a "dieback" [*Cox et al.*, 2000, 2004], especially in northeastern parts, with MPI-ESM-LR having the largest decrease in carbon drawdown (also seen in *Giorgetta et al.* [2013]) of −10% to −20%. The Amazon dieback in MPI-ESM-LR is reversed under MSB (Figure 2). The carbon to nitrogen ratio could be a limiting factor in the areas with reduced GPP in NorESM1-M, as this has been shown to be an important process in this model [*Thornton et al.*, 2007].

There is an increase in GPP overall in the 2060s in G3-seaSalt compared to RCP4.5 in the 2010s (Figures 4c and 4d), likely owing to the carbon fertilization, as photosynthesis is enhanced under higher CO_2 levels [*Farquhar*, 1997]. The increase is less than without MSB, however, in NorESM1-M and IPSL-CM5A-LR. The sustained carbon fertilization effect shown by models [e.g., *Bonan*, 2008; *Friedlingstein et al.*, 2006; *Denman et al.*, 2007] is not entirely supported by observations [*Canadell et al.*, 2007; *Norby et al.*, 2010]. Hence, the modeled GPP values might be overestimated, though uncertainties remain concerning this issue.

3.4. The Potential Importance of Salt Effects on Vegetation

There is a substantial increase in the load of sea salt in the lowest atmospheric level in the final decade of MSB in NorESM1-M (the only model that output this nonstandard CMIP5 variable) (Figure 5). After the emissions of sea salt at the sea surface, this is the amount that is transported up into the atmospheric lowest level. Over the tropical land areas, there is an increase of more than 200%, reaching as much as 600% in places (Figure 5a). The effects of salt on vegetation are not included in the models but could be an important factor under this climate engineering technique. Salt stress on plants can affect all major processes, including photosynthesis, protein synthesis, and energy and lipid metabolism [*Parida and Das*, 2005; *Qadir et al*., 2014].

4. Conclusions

The tropical gross primary productivity has been investigated in three Earth system models in a future scenario with climate engineering in the form of marine sky brightening. The model response is diverse, with two models showing an overall reduction in the gross drawdown of carbon by tropical rainforests from the atmosphere are found compared to a nonengineered climate. The fluxes are still higher than the simulated values for the 2010s, however, most likely from the carbon fertilization effect in the models. Nitrogen availability could become a future limiting factor, as suggested by NorESM1-M, the only model to include this effect. GPP shows a positive partial correlation to precipitation in the Amazon and Africa in NorESM1-M and in Amazon in IPSL-CM5A-LR in the 2060s. Any circulation changes leading to changes to precipitation patterns in the tropics are not only important under future climate change but also under any future climate engineering, should society ever decide to implement any such techniques. Dieback of the Amazon rainforest found in the MPI-ESM-LR RCP4.5 simulation [*Giorgetta et al*., 2013] is recovered by MSB. This GPP increase in the G3-seaSalt simulation is partially correlated to a temperature reduction. Southwestern Amazon GPP increases in IPSL-CM5A-LR are also correlated to cooler temperatures.

Marine sky brightening could result in wind-driven spread of sea salt onto land and hence be detrimental to plant productivity and furthermore cause corrosion of infrastructure. An increase in the load of sea salt in the atmosphere over tropical land of as much as 600% was seen in the final decade of MSB. We suggest that the effects of salt on vegetation and soils should be included in land surface and vegetation models.

The tropics are particularly challenging for models to simulate well as the coupling between the water cycle and circulation is especially reliant on unresolved processes, mainly related to clouds. The cloud parameterizations further influence the modeling and impacts of the particular climate engineering method evaluated here. The response of the climate, including tropical forests, to MSB is therefore inherently uncertain. Only three models were compared in this study, showing a diversity in response; and to further our understanding, the results from the ongoing GeoMIP sea spray climate engineering experiments will be valuable [*Kravitz et al*., 2013]. The lack of a robust response among the models, with regards to the sign of change as well as the cause, indicates that the rainforest is potentially vulnerable to the regional and seasonal climate changes from climate engineering and that the response is highly uncertain.

Acknowledgments
This work is supported by the European Commission's 7th Framework Programme (FP7) projects IMPLICC (FP7-ENV-2008-1-226567). H.M. is funded by the Norwegian Research Council project EXPECT (grant 229760/E10), and computing time was provided by NOTUR. The MPI-ESM-LR simulations were performed and archived at DKRZ. U.N. is founded by the German Science Foundation special priority program 1689 in project CEIBRAL. The IPSL-CM5A-LR model simulations were performed with the HPC resources of (CCRT/TGCC/CINES/IDRIS) under the allocation 2012-t2012012201 made by GENCI (Grand Equipement National de Calcul Intensif), CEA (Commissariat à l'Energie Atomique et aux Energies Alternatives), and CNRS (Centre National de la Recherche Scientifique). The data are available on the Earth System Grid (http://esgf-data.dkrz.de/esgf-web-fe/) and from DKRZ (http://implicc1.dkrz.de:8080/thredds/catalog.html). We would like to thank Chris Jones, one anonymous reviewer, and the Editor for helpful comments.

The Editor thanks Christopher Jones and an anonymous reviewer for their assistance in evaluating this paper.

References

Alterskjær, K., J. E. Kristjánsson, O. Boucher, H. Muri, U. Niemeier, H. Schmidt, M. Schulz, and C. Timmreck (2013), Sea-salt injections into the low-latitude marine boundary layer: The transient response in three Earth system models, *J. Geophys. Res. Atmos.*, *118*, 12,195–12,206, doi:10.1002/2013JD020432.

Anav, A., P. Friedlingstein, M. Kidston, L. Bopp, P. Ciais, P. Cox, C. Jones, M. Jung, R. Myneni, and Z. Zhu (2013), Evaluating the land and ocean components of the global carbon cycle in the CMIP5 Earth system models, *J. Clim.*, *26*(18), 6801–6843.

Beer, C., et al. (2010), Terrestrial gross carbon dioxide uptake: Global distribution and covariation with climate, *Science*, *329*(5993), 834–838.

Bentsen, M., et al. (2013), The Norwegian Earth System Model, NorESM1-M—Part 1: Description and basic evaluation of the physical climate, *Geosci. Model Dev.*, *6*(3), 687–720.

Boer, G. J., and V. Arora (2010), Geographic aspects of temperature and concentration feedbacks in the carbon budget, *J. Clim.*, *23*(3), 775–784.

Bonan, G. B. (2008), Forests and climate change: Forcings, feedbacks, and the climate benefits of forests, *Science*, *320*(5882), 1444–1449, doi:10.1126/science.1155121.

Bonan, G. B., S. Levis, L. Kergoat, and K. W. Oleson (2002), Landscapes as patches of plant functional types: An integrating concept for climate and ecosystem models, *Global Biogeochem. Cycles*, *16*(2), 1021, doi:10.1029/2000GB001360.

Canadell, J. G., C. Le Quéré, M. R. Raupach, C. B. Field, E. T. Buitenhuis, P. Ciais, T. J. Conway, N. P. Gillett, R. A. Houghton, and G. Marland (2007), Contributions to accelerating atmospheric CO_2 growth from economic activity, carbon intensity, and efficiency of natural sinks, *Proc. Natl. Acad. Sci. U.S.A.*, *104*(47), 18,866–18,870, doi:10.1073/pnas.0702737104.

Cheng, W., D. A. Sims, Y. Luo, J. S. Coleman, and D. W. Johnson (2000), Photosynthesis, respiration, and net primary production of sunflower stands in ambient and elevated atmospheric CO_2 concentrations: An invariant NPP:GPP ratio?, *Global Change Biol.*, *6*(8), 931–941.

Cook, K. H., and E. K. Vizy (2006), Coupled model simulations of the West African monsoon system: Twentieth- and twenty-first-century simulations, *J. Clim.*, *19*(15), 3681–3703.

Cox, P. M., R. A. Betts, C. D. Jones, S. A. Spall, and I. J. Totterdell (2000), Acceleration of global warming due to carbon-cycle feedbacks in a coupled climate model, *Nature*, *408*, 184–187.

Cox, P. M., R. A. Betts, M. Collins, P. P. Harris, C. Huntingford, and C. D. Jones (2004), Amazonian forest dieback under climate-carbon cycle projections for the 21st century, *Theor. Appl. Climatol.*, *78*(1–3), 137–156.

Denman, K. L., et al. (2007), Contribution of working group I to the fourth assessment report of the Intergovernmental Panel on Climate Change, in *Climate Change, The Physical Science Basis*, edited by S. Solomon et al., pp. 499–587, Cambridge Univ. Press, Cambridge, U. K.

Dufresne, J. L., et al. (2013), Climate change projections using the IPSL-CM5 Earth System Model: From CMIP3 to CMIP5, *Clim. Dyn.*, *40*(9–10), 2123–2165.

Dukes, J. S., N. R. Chiariello, E. E. Cleland, L. A. Moore, M. R. Shaw, S. Thayer, T. Tobeck, H. A. Mooney, and C. B. Field (2005), Responses of grassland production to single and multiple global environmental changes, *PLoS Biol.*, *3*(10), e319.

Farquhar, G. D. (1997), Carbon dioxide and vegetation, *Science*, *278*(5342), 1411, doi:10.1126/science.278.5342.1411.

Field, C. B., R. B. Jackson, and H. A. Mooney (1995), Stomatal responses to increased CO_2: Implications from the plant to the global scale, *Plant Cell Environ.*, *18*(10), 1214–1225, doi:10.1111/j.1365-3040.1995.tb00630.x.

Friedlingstein, P., et al. (2006), Climate-carbon cycle feedback analysis: Results from the C^4MIP model intercomparison, *J. Clim.*, *19*(14), 3337–3353.

Giorgetta, M. A., et al. (2013), Climate and carbon cycle changes from 1850 to 2100 in MPI-ESM simulations for the Coupled Model Intercomparison Project phase 5, *J. Adv. Model. Earth Syst.*, *5*(3), 572–597, doi:10.1002/jame.20038.

Huete, A. R., K. Didan, Y. E. Shimabukuro, P. Ratana, S. R. Saleska, L. R. Hutyra, W. Yang, R. R. Nemani, and R. Myneni (2006), Amazon rainforests green-up with sunlight in dry season, *Geophys. Res. Lett.*, *33*, L06405, doi:10.1029/2005GL025583.

Hurtt, G. C., et al. (2011), Harmonization of land-use scenarios for the period 1500–2100: 600 years of global gridded annual land-use transitions, wood harvest, and resulting secondary lands, *Clim. Change*, *109*(1–2), 117–161.

Jones, A., and J. M. Haywood (2012), Sea-spray geoengineering in the HadGEM2-ES earth-system model: Radiative impact and climate response, *Atmos. Chem. Phys.*, *12*(22), 10,887–10,898.

Jones, A., J. M. Haywood, and O. Boucher (2009), Climate impacts of geoengineering marine stratocumulus clouds, *J. Geophys. Res.*, *114*, D10106, doi:10.1029/2008JD011450.

Jones, A., J. M. Haywood, and O. Boucher (2011), A comparison of the climate impacts of geoengineering by stratospheric SO_2 injection and by brightening of marine stratocumulus cloud, *Atmos. Sci. Lett.*, *12*(2), 176–183.

Jung, M., et al. (2011), Global patterns of land-atmosphere fluxes of carbon dioxide, latent heat, and sensible heat derived from eddy covariance, satellite, and meteorological observations, *J. Geophys. Res.*, *116*, G00J07, doi:10.1029/2010JG001566.

Kitoh, A., H. Endo, K. Krishna Kumar, I. F. A. Cavalcanti, P. Goswami, and T. Zhou (2013), Monsoons in a changing world: A regional perspective in a global context, *J. Geophys. Res. Atmos.*, *118*, 3053–3065.

Korhonen, H., K. S. Carslaw, and S. Romakkaniemi (2010), Enhancement of marine cloud albedo via controlled sea spray injections: A global model study of the influence of emission rates, microphysics and transport, *Atmos. Chem. Phys.*, *10*(9), 4133–4143.

Kravitz, B., A. Robock, O. Boucher, H. Schmidt, K. E. Taylor, G. Stenchikov, and M. Schulz (2011), The geoengineering model intercomparison project (GeoMIP), *Atmos. Sci. Lett.*, *12*(2), 162–167.

Kravitz, B., et al. (2013), Sea spray geoengineering experiments in the geoengineering model intercomparison project (GeoMIP): Experimental design and preliminary results, *J. Geophys. Res. Atmos.*, *118*, 11,175–11,186, doi:10.1002/jgrd.50856.

Krinner, G., N. Viovy, N. de Noblet-Ducoudré, J. Ogée, J. Polcher, P. Friedlingstein, P. Ciais, S. Sitch, and I. C. Prentice (2005), A dynamic global vegetation model for studies of the coupled atmosphere-biosphere system, *Global Biogeochem. Cycles*, *19*, GB1015, doi:10.1029/2003GB002199.

Latham, J. (1990), Control of global warming?, *Nature*, *347*(6291), 339–340.

Lawrence, D. M., et al. (2011), Parameterization improvements and functional and structural advances in Version 4 of the Community Land Model, *J. Adv. Model. Earth Syst.*, *3*(3), M03001, doi:10.1029/2011MS000045.

Lewis, S. L., et al. (2009), Increasing carbon storage in intact African tropical forests, *Nature*, *457*(7232), 1003–1006 doi:10.1038/nature07771.

Le Quéré, C., et al. (2009), Trends in the sources and sinks of carbon dioxide, *Nat. Geosci.*, *2*, 831–836, doi:10.1038/ngeo689.

Le Quéré, C., et al. (2014), Global carbon budget 2014, *Earth Syst. Sci. Data Discuss.*, *7*, 521–610, doi:10.5194/essdd-7-521-2014.

Mercado, L. M., N. Bellouin, S. Sitch, O. Boucher, C. Huntingford, M. Wild, and P. M. Cox (2009), Impact of changes in diffuse radiation on the global land carbon sink, *Nature*, *458*, 1014–1017, doi:10.1038/nature07949.

Niemeier, U., H. Schmidt, K. Alterskjær, and J. E. Kristjánsson (2013), Solar irradiance reduction via climate engineering: Impact of different techniques on the energy balance and the hydrological cycle, *J. Geophys. Res. Atmos.*, *118*, 11,905–11,917, doi:10.1002/2013JD020445.

Norby, R. J., and D. R. Zak (2011), Ecological lessons from Free-Air CO_2 Enrichment (FACE) experiments, *Annu. Rev. Ecol. Evol. Syst.*, *42*, 181–203.

Norby, R. J., et al. (2005), Forest response to elevated CO_2 is conserved across a broad range of productivity, *Proc. Natl. Acad. Sci. U.S.A.*, *102*(50), 18,052–18,056.

Norby, R. J., J. M. Warren, C. M. Iversen, B. E. Medlyn, and R. E. McMurtrie (2010), CO_2 enhancement of forest productivity constrained by limited nitrogen availability, *Proc. Natl. Acad. Sci. U.S.A.*, *107*(45), 19,368–19,373.

Nowak, R. S., D. S. Ellsworth, and S. D. Smith (2004), Functional responses of plants to elevated atmospheric CO_2—Do photosynthetic and productivity data from FACE experiments support early predictions?, *New Phytol.*, *162*(2), 253–280.

Oleson, K. W., et al. (2010), Technical description of version 4.0 of the Community Land Model (CLM), *Tech. Rep.*, *NCAR/TN-478+STR*, Natl. Cent. for Atmos. Res., Boulder, Colo.

Parida, A. K., and A. B. Das (2005), Salt tolerance and salinity effects on plants: A review, *Ecotoxicol. Environ. Saf.*, *60*(3), 324–349.

Phillips, R. P., I. C. Meier, E. S. Bernhardt, A. S. Grandy, K. Wickings, and A. C. Finzi (2012), Roots and fungi accelerate carbon and nitrogen cycling in forests exposed to elevated CO_2, *Ecol. Lett.*, *15*, 1042–1049, doi:10.1111/j.1461-0248.2012.01827.x.

Piao, S., P. Ciais, P. Friedlingstein, N. de Noblet-Ducoudré, P. Cadule, N. Viovy, and T. Wang (2009), Spatiotemporal patterns of terrestrial carbon cycle during the 20th century, *Global Biogeochem. Cycles*, *23*, GB4026, doi:10.1029/2008GB003339.

Poulter, B., P. Ciais, E. Hodson, H. Lischke, F. Maignan, S. Plummer, and N. E. Zimmermann (2011), Plant functional type mapping for earth system models, *Geosci. Model Dev.*, *4*, 993–1010, doi:10.5194/gmd-4-993-2011.

Qadir, M., E. Quillérou, V. Nangia, G. Murtaza, M. Singh, R. J. Thomas, P. Drechsel, A. D. Noble (2014), Economics of salt-induced land degradation and restoration, *Natural Resources Forum* (*accepted*). 27 pp. [Available at http://hdl.handle.net/11375/15697.]

Raddatz, T. J., C. H. Reick, W. Knorr, J. Kattge, E. Roeckner, R. Schnur, K. G. Schnitzler, P. Wetzel, and J. Jungclaus (2007), Will the tropical land biosphere dominate the climate-carbon cycle feedback during the twenty-first century?, *Clim. Dyn.*, *29*(6), 565–574.

Rutishauser, E., D. Barthélémy, L. Blanc, and N. Eric-André (2011), Crown fragmentation assessment in tropical trees: Method, insights and perspectives, *For. Ecol. Manage.*, *261*(3), 400–407.

Saleska, S. R., K. Didan, A. R. Huete, and H. R. da Rocha (2007), Amazon forests green-up during 2005 drought, *Science*, *318*(5850), 612, doi:10.1126/science.1146663.

Shaw, M. R., E. S. Zavaleta, N. R. Chiariello, E. E. Cleland, H. A. Mooney, and C. B. Field (2002), Grassland responses to global environmental changes suppressed by elevated CO_2, *Science*, *298*(5600), 1987–1990.

Taylor, K. E., R. J. Stouffer, and G. A. Meehl (2011), An overview of CMIP5 and the experiment design, *Bull. Am. Meteorol. Soc.*, *93*(4), 485–498.

Thornton, P. E., J.-F. Lamarque, N. A. Rosenbloom, and N. M. Mahowald (2007), Influence of carbon-nitrogen cycle coupling on land model response to CO_2 fertilization and climate variability, *Global Biogeochem. Cycles*, *21*, GB4018, doi:10.1029/2006GB002868.

Tjoelker, M. G., J. Oleksyn, and P. B. Reich (1999), Acclimation of respiration to temperature and CO_2 in seedlings of boreal tree species in relation to plant size and relative growth rate, *Global Change Biol.*, *5*(6), 679–691.

Whittaker, R. H. (1975), *Communities and Ecosystems*, Macmillan, New York.

Wolkovich, E. M., et al. (2012), Warming experiments underpredict plant phenological responses to climate change, *Nature*, *485*(7399), 494–497.